High Speed Data Transmission on Small Gauge Cables for the ATLAS Pixel Upgrade

J. Shahinian, J. Volk, V. Fadeyev, A.A. Grillo, B. Meimban, J. Nielsen, M. Wilder
Santa Cruz Institute for Particle Physics
University of California Santa Cruz

ABSTRACT

Data transmission requirements for the upgrade of the ATAS Pixel detector will be difficult to meet. The expected trigger rate and occupancy imply multi-gigabit per second transmission rates will be required but radiation levels immediately at the detector preclude completely optical solutions. Electrical transmission for a short distance will be necessary to move optical components to a safer area. We have evaluated electrical transmission over short distances to determine the minimum size cable capable of 1-5 Gbps bandwidth. Test results indicate multi-gigabit bandwidth is achievable with very thin cables. Results for various low-mass cable configurations and bandwidths are presented.

INTRODUCTION

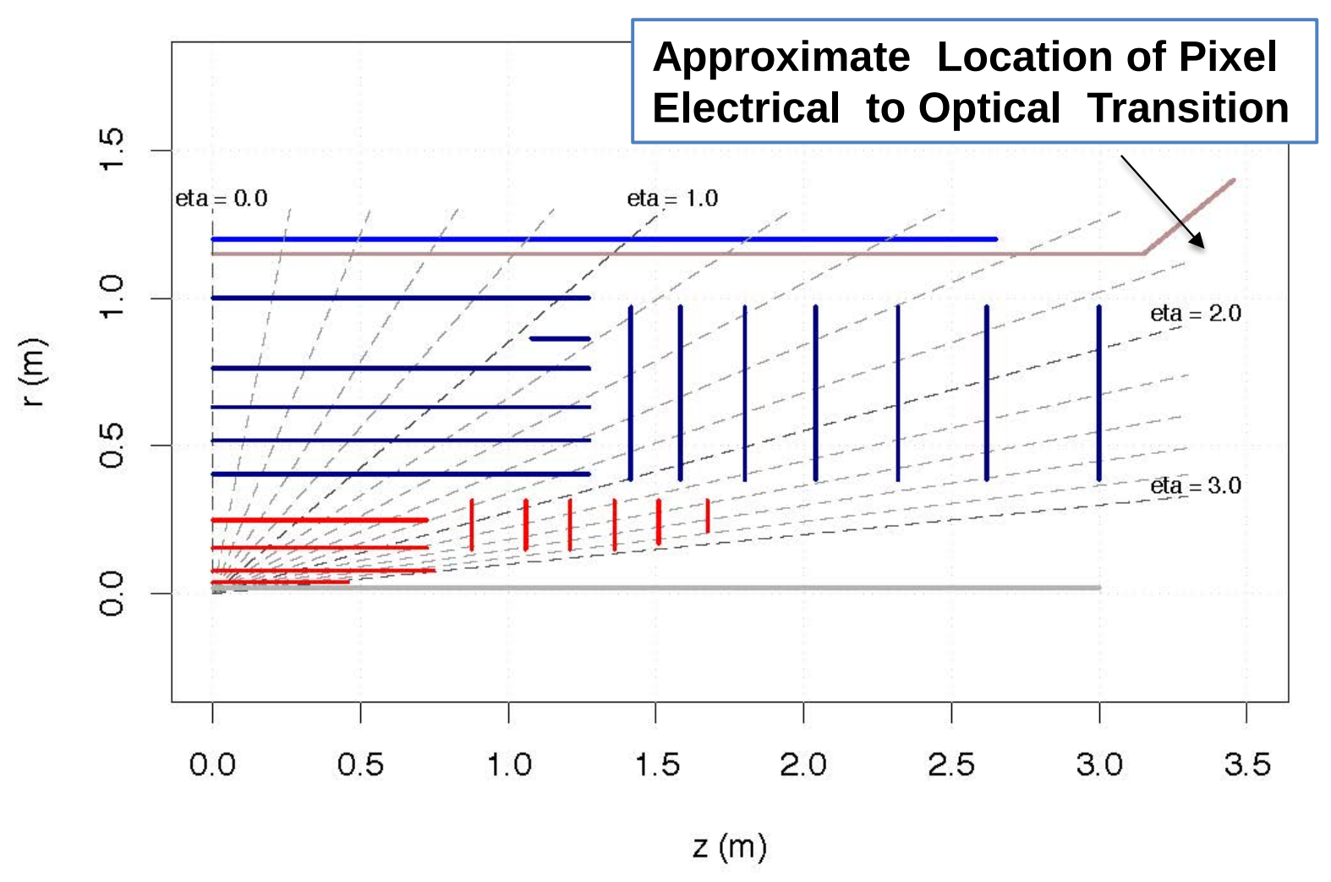

Figure 1 (Above). Graph shows the positions of the Silicon Pixel and Silicon Strip detector layers from the ATLAS Letter of Intent (LOI) Dec-2012. The cross-section view of only one quadrant is shown with the interaction point at (0,0). Pixel barrel and end-cap layers are shown in red, Strips in blue.

Figure 2 (Below). Table lists the radii of each Pixel Barrel layer, their half-length and the expected required bandwidth for each detector module on each layer.

Detector:	Radial Position [mm]	Stave Half-Length [mm]	Staves	Modules /Stave	Module Type	Rate/Module [Gb/s]
Layer 1	39	456.5	16	22	dual	5.12
Layer 2	78	747	16	36	quad	5.12
Layer 3	155	722.8	32	35	quad	2.56
Layer 4	250	722.8	52	35	quad	1.28

The Pixel detector for the planned Phase II upgrade to the ATLAS detector will sit closest to the interaction region as shown in Figure 1. The large number of tracks per bunch crossing in this region will require very high segmentation that is small pixel size, and consequently **very high data rates** to be transmitted off detector. As can be seen in Table 1, the required bandwidth per layer (e.g. modules/stave X Rate/Module) could exceed 100 Gb/s, possibly exceeding even optical transmission technology. The plan then is to segment the data transmission into separate links from each module.

The two other serious constraints are the **high radiation environment** of the Pixel detector and **the need to minimize material** in the tracking volume in order to minimize scattering and energy loss of the particles being measured. The radiation environment could reach levels up to 10 MGray, well above the tolerance of any optical devices presently identified. Thus, **electrical transmission is required for several meters** before a transition to optical can be made in an area with lower radiation levels. The design goal then is to find an electrical transmission medium that can meet the necessary bandwidth with the least mount of material. Bandwidth vs. distance, error rates, and cross-talk were tested for several cable configurations of various material structures, whose guided selection evolved with the experimental process (Figure 3). As most of the cable's radiation length is in its shield rather than in its inner conductor or dielectric, unshielded twisted pair was the first choice given its general immunity to interference as well as low mass.

We found, however, that a twisted pair cable could be designed with a custom thin shield with very little material penalty and the inclusion of the shield yielded a more convenient cable impedance and contributed to more mechanical stability.

Multi-gigabit per second data rates expected in transmission lines warrants caution to non-linear high-frequency signal-degrading electrical phenomena, such as skin effect and dielectric loss tangent. Equations 1-4[1] show the relationship between skin effect resistance, frequency, impedance, and Attenuation and Bandwidth limitations due to cable length and losses, in the skin effect and dielectric loss regimes:

$$\boldsymbol{R_{SKIN}} \propto \sqrt{\boldsymbol{\omega}} \qquad \text{[Eq. 1]}$$

$$Z = \sqrt{\frac{j\omega L+\boldsymbol{R_{DC}}+\boldsymbol{R_{SKIN}}}{j\omega C}} \qquad \text{[Eq. 2]}$$

$$Attenuation_{SKIN} \propto \sqrt{\boldsymbol{\omega}} \qquad Attenuation_{DIELECTRIC} \propto \boldsymbol{\omega} \qquad \text{[Eq. 3]}$$

$$BW_{SKIN} \propto {}^{1}/_{L^2} \qquad BW_{DIELECTRIC} \propto {}^{1}/_{L} \qquad \text{[Eq. 4]}$$

X0 at Z~=0 (1Link)/X0 at EOS Layer 1 (11Links)/X0 at EOS Layer 2 (19LInks)				
0.032%/5.13%/8.86%	0.023%/3.55%/6.14%	0.0086%/1.35%/2.33%	0.003%/0.47%/0.82%	0.021%/3.24%/5.6%

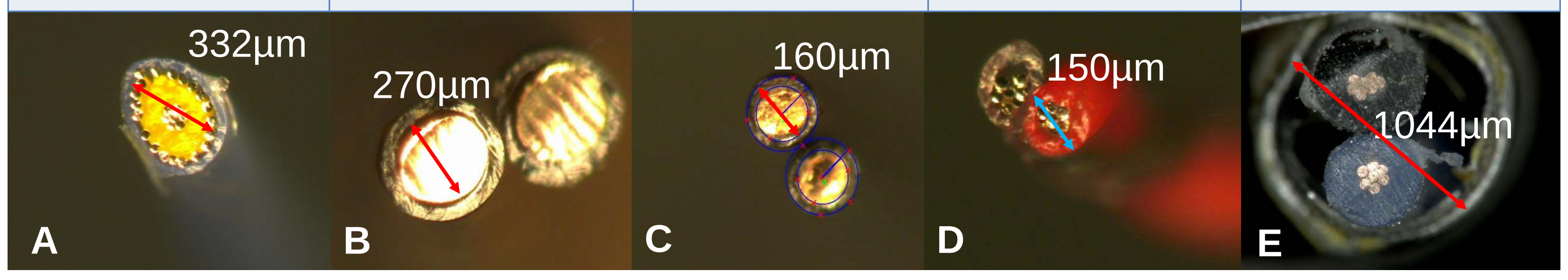

Figure 3 (Above). Transmission lines tested in differential configuration; from left to right, and their anticipated X0 in each EOS layer, based on cable size and path route: **(A)** Two 1m-long sections of 42AWG 50Ω Axon PCX 42K10 coax cable. **(B)** 75Ω 32AWG Kapton (polyimide)-insulated solid core twisted pair. **(C)** 75Ω 36AWG Kapton-insulated solid-core twisted pair. **(D)** 50Ω fluoropolymer-insulated stranded Ag-plated Cu-core twisted pair. **(E)** 50Ω PEEK-insulated stranded-core twisted pair with Al-foil shield—custom twisted pair.

CHARACTERIZATION

RocketIO Multigigabit Transceiver ML405 FPGA from Xilinx was used as a differential cable Bit-Error Rate Tester (BERT) to measure bandwidths up to 6.22Gbps with compensation techniques such as 8b/10b encoding and pre-emphasis. Error rates $<10^{-13}$ were sought and cable bandwidths documented in Figure (4) were those at which occurrences of errors were 10^{-13} or less.

Figure 4 (Below). Experimentally-determined bandwidths of twisted pairs labeled as C, D, E in Figure 3 as a function of length, from the BERT tester. Available bandwidth decreases with length, as could be expected from Eq. 4. We only show useful (payload) bandwidth in cases when 8/10b encoding is used.

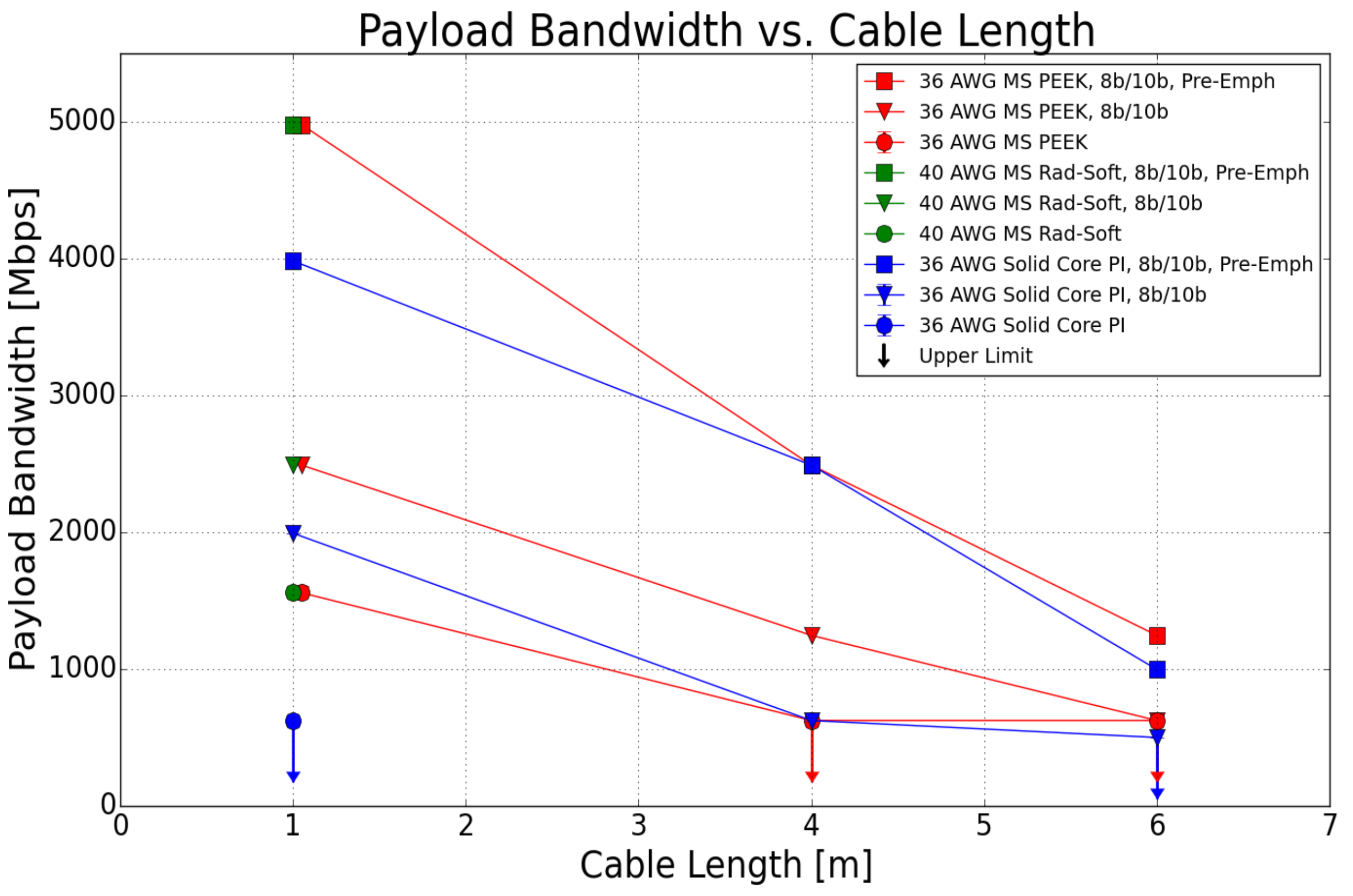

Custom transmission line was manufactured by Dacon Systems, Inc. (Corona, CA): 100Ω multi-strand conductor twisted pair with Poly-Ether-Ether-Ketone (PEEK) insulation and Al shield. PEEK dielectric is known from previous studies to (i.) have a low dielectric loss tangent[3] and (ii.) maintain its integrity after irradiation[2], so the custom-made twisted pair promises radiation hardness to the expected dose; however, this projection must be verified.

The data in Figure 4 show that the twisted pair bandwidth is acceptable over a short distance but does not meet our requirements at the necessary cable length of 7m. A solution could be a hybrid cable composed of shielded twisted pair to run along inner-detector barrels then transition to twinax cable to reach the safe area for optical components further from the detectors (Figure 1). Figure 5 shows that such cable indeed handles the high bandwidth.

CHARACTERIZATION (CT' D.)

Crosstalk

Figure 5 (Right). Bandwidth of cable affected by crosstalk. Self-induced crosstalk was simulated by winding the transmission line around non-conducting spools of various sizes. All cables had a thin shield.

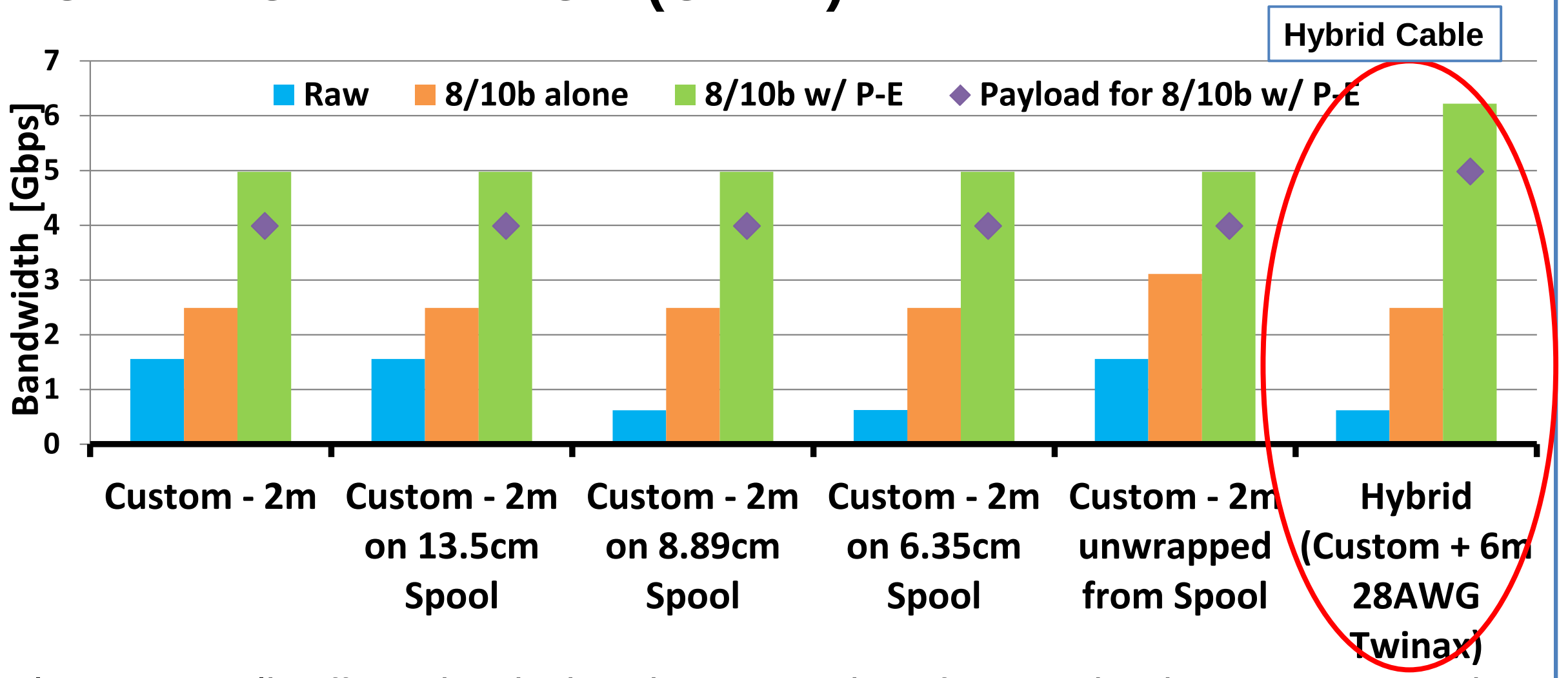

Differential cable in general exhibits low cross-talk effects by design; however when frequencies increase, even short lengths along a cable can become small antennas susceptible to pickup. Victim twisted pair lying next to aggressor twisted pair in environmental conditions similar to those in the detector — against a prototype carbon-fiber I-beam on which the modules will be mounted (Figure 6) — can simulate cross-talk effects.

Figure 6, 7. (Left, Below) Modules will be mounted on Carbon-Fiber I-beam (LBNL) and provide reasonable testing environment for Transmission line cross-talk.

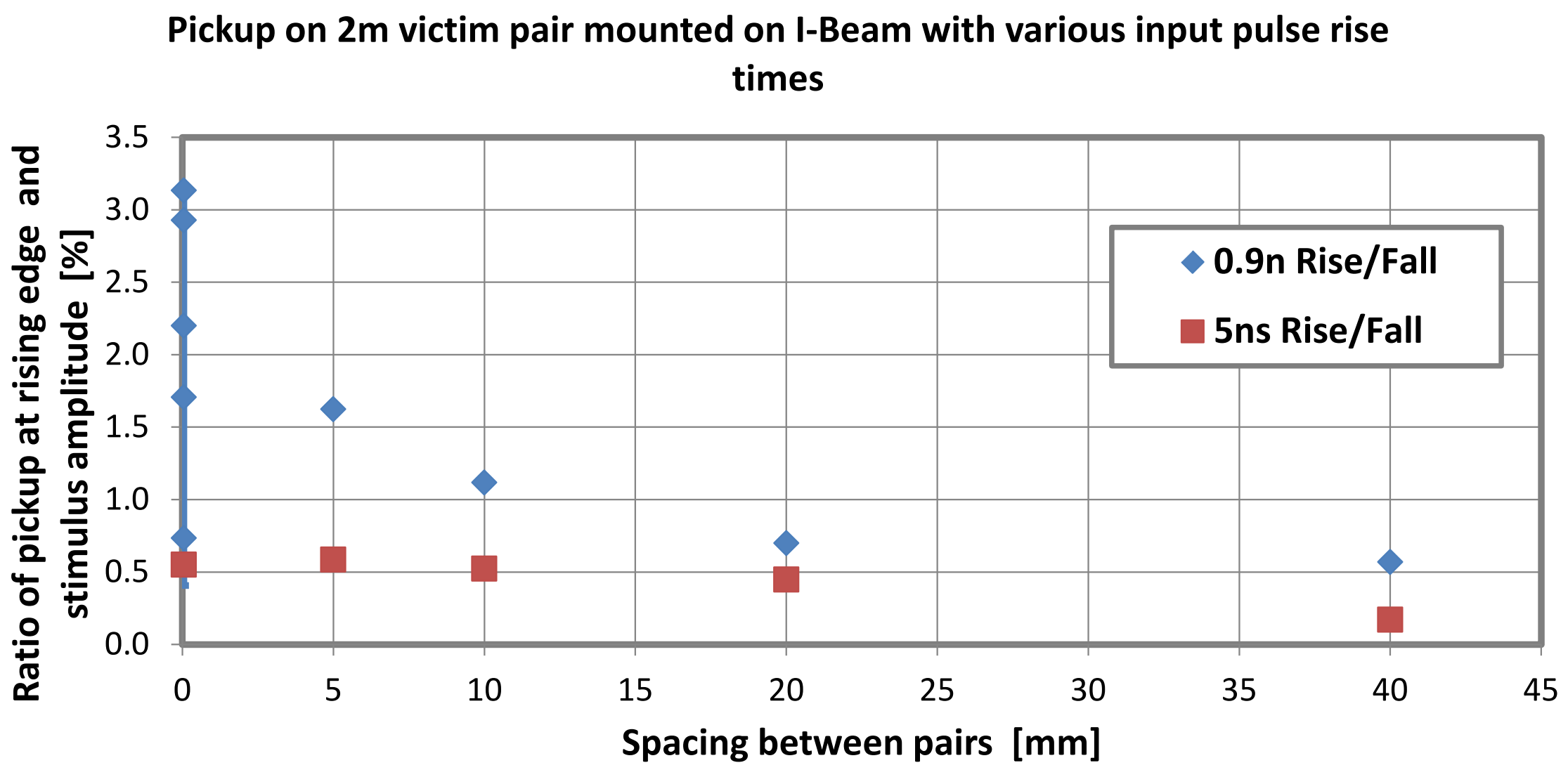

Figure 8. (Above) Measurements of cross talk on victim twisted pair as a function of distance from the aggressor twisted pair. Different driving conditions were tested while keeping the aggressor signal amplitude at 800 mV. A 2m custom twisted pair was investigated here.

Shortest driving pulse rise time indicates highest driving frequency, and the least desirable amount of cross talk.

Skin Effect

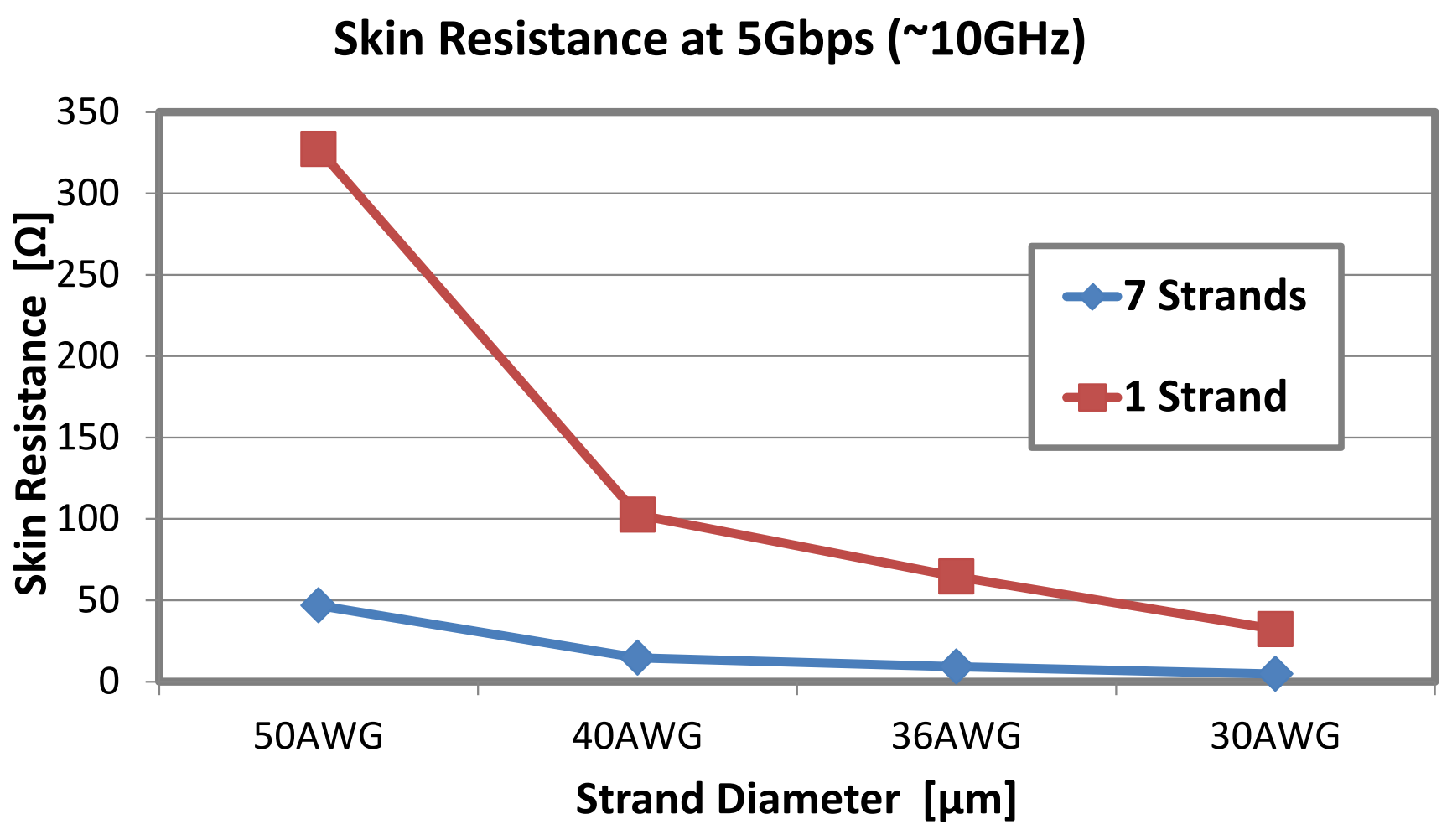

Figure 9. (Left) Estimated Resistance due to skin effect at 10GHz with solid-conductor and multi-strand conductor cores.

Modeling

Models are based upon a 4-port scattering matrix solution, an extension of the 2-port model (Figure 10), which quantifies a cable's termination properties based on load-matching at high frequencies. S-parameters of the cable under test were measured with a 2-port spectrum analyzer and used for simulation in Agilent's Advanced Design System software.

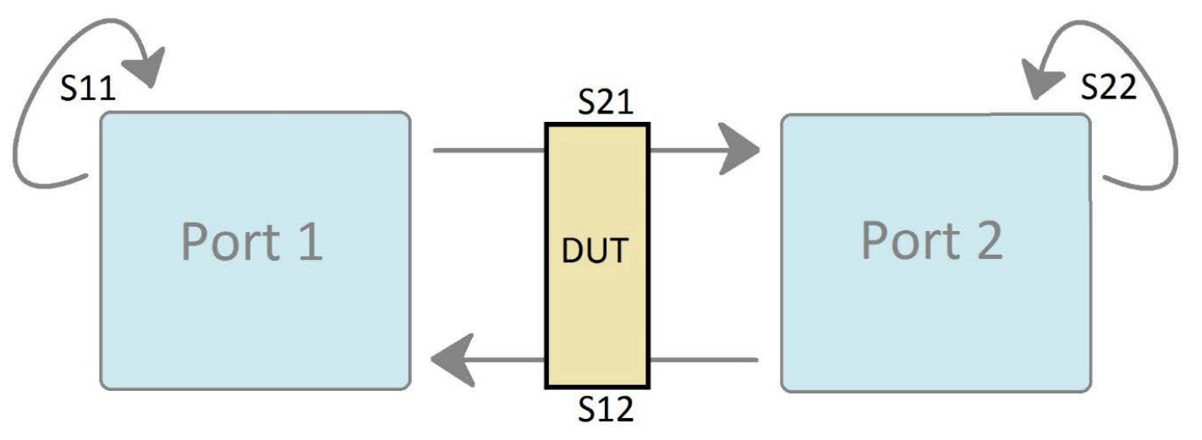

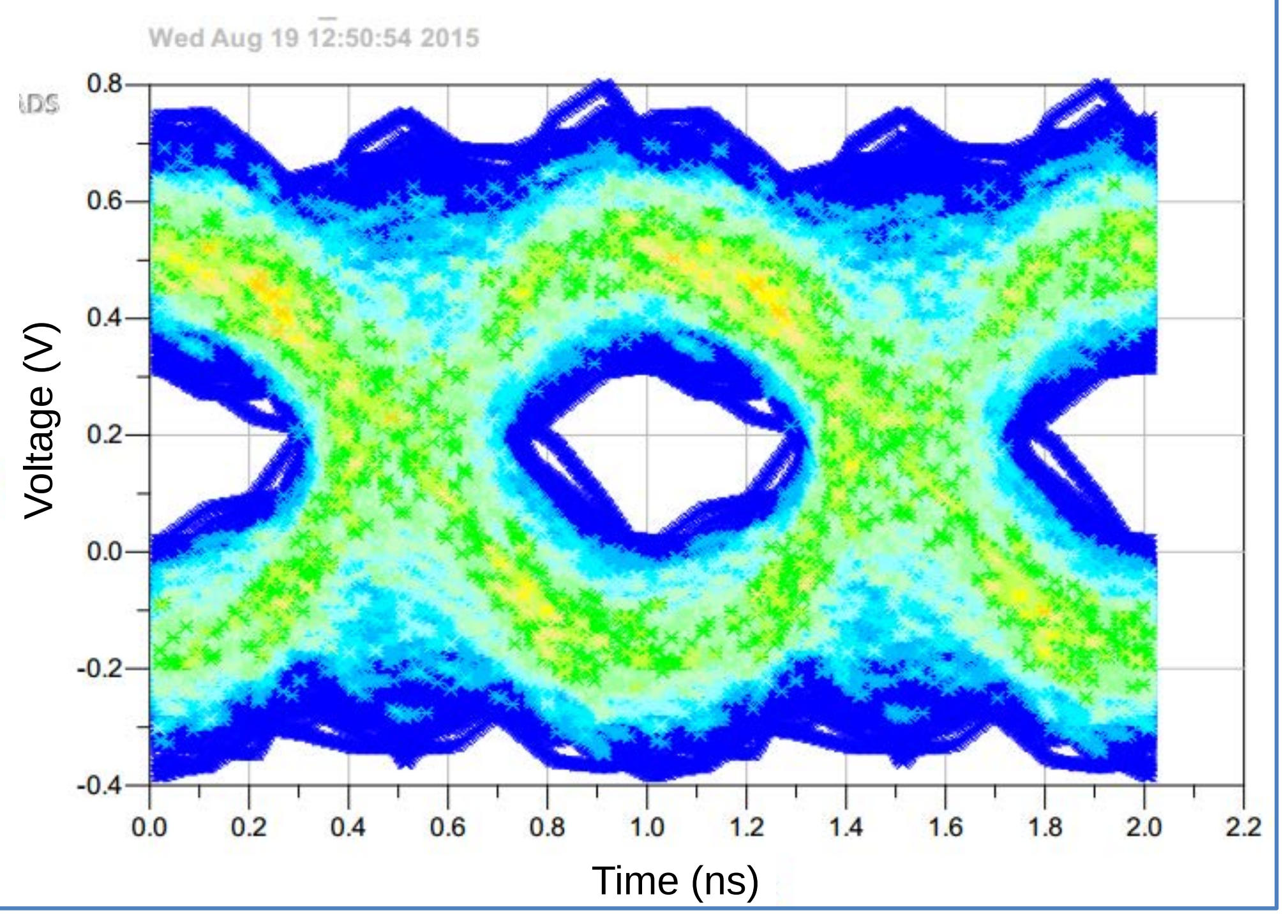

Figure 10 (Above). 2-port S-parameters generate a 2x2 matrix of parameters characteristic of the transmission line under test; it follows that 4-port S-parameters in a differential system generate a 4x4 matrix.
Figure 11 (Right). Eye diagram of 1m 36AWG PEEK (Custom) twisted pair simulated in Agilent's Advanced Design System software based on S-parameter measurements.

CONCLUSIONS

We have successfully demonstrated that transmission lines with sub-200 µm conductive-core diameter can effectively transmit data at relatively high speeds. The most promising rates achieved with stranded conductor cores, especially if the conductors are plated with lower-resistance metal; however, due to the increased activation caused by the plating, this option is not feasible for application. For as much consistency in line performance as practically achievable from the lab to site destination, we think that cable shielding is necessary. We made a custom twisted pair cable with multi-stranded conductors, PEEK insulation and thin Al shield. It exhibits promising performance of 5 Gbps payload transmission speed at 1 m length. This transmission speed can be extended to 7 m total length by connecting it to 6 m twinax cable.

FUTURE WORK

Most remaining work is in radiation characterization of the more suitable transmission lines. This includes investigating the mechanical degradation and the transmission quality after radiation. Due to the large quantity of lines needed for each stave, an efficient and reliable electrical 'quick' connector is desired and will similarly be researched. A third aspect to pursue is the final transmission line routing configuration, including the full transmission chain from the front-end chip to carrier flex circuit to the transmission cable. A further miniaturization of the cable is of interest as well.

A final investigation is warranted for crosstalk amongst many cables. In practice, only one cable was driven at any time and a nearby cable probed for pickup. In a non-isolated system, where many cables are transmitting high-frequency data, we need to confirm that significantly more cross-talk or interference does not result. In particular, the imperviousness of a differential configuration to crosstalk under these conditions is of interest.

ACKNOWLEDGMENTS

We thank Maurice Garcia-Sciveres for stimulating discussions and for providing a prototype I-beam structures. We thank Su Dong and Martin Kocian for providing BERT system and twinax cable samples. We thank Neil McFadden, Martin Hoeferkamp, and Sally Seidel for cable irradiations and useful discussions. This work was supported by Department of Energy, grant DEFG02-13ER41983.

References

1) Johnson, H. Graham, M. (06 Mar. 2003) "High-Speed Signal Propagation: Advanced Black Magic". *Print*. Ed. Upper Saddle River, NJ: Prentice Hall.
2) Idesaki, A. et. al. (02 Oct. 2012) "Evaluation of Radiation Resistance for Organic Materials Used in Atomic Energy-related Facilities." *Web.* Japan Atomic Energy Agency (JAEA). Quantum Beam Science Directorate. Advanced Ceramic Group. Takasaki Advanced Radiation Research Institute (TARRI).
3) "Dielectric Properties of PEEK^{TM} Polymer." (07 Aug. 2014) *Web*. CG TEC. *cgtec.eu*. Accessed 16 Aug. 2015.

TWEPP 2015 – Topical workshop on Electronics for Particle Physics, Lisbon, Portugal